Kaolinites structural defects related to urea and dimethyl sulfoxide intercalation

Hervé Barye Tatang, Jean Aimé Mbey, Cyrill Joël Ngally Sabouang, Jacques Richard Mache, Renaud Gley, Sakeo Kong

Kaolinite structural defects related to urea and dimethyl sulfoxide intercalation

Hervé Barye TATANG[1], Jean Aimé MBEY[1*], Cyrill Joël NGALLY SABOUANG[2], Jacques Richard MACHE[3], Renaud GLEY[4], Sakeo KONG[1]

[1] Laboratory of Applied Inorganic Chemistry, Department of Inorganic Chemistry, University of Yaoundé I, P.O. Box 812 Yaoundé.

[2] Department of Chemistry, Higher Teacher Training College, University of Bamenda, P.O. Box 39, Bambili, Cameroon.

[3] School of Geology and Mining Engineering, University of Ngaoundere, P.O. Box 115, Meiganga, Cameroon.

[4] Laboratoire Interdisciplinaire des Environnements Continentaux (LIEC), Université de Lorraine, CNRS, UMR 7360, F-54000 Nancy, France.

J. A. MBEY: mbey25@yahoo.fr; jean-aime.mbey@facsciences-uy1.cm

H. B. TATANG: hervebarye@gmail.com/barye.tatang@facsciences-uy1.cm

* Correspondence: mbey25@yahoo.fr; jean-aime.mbey@facsciences-uy1.cm

PO BOX 812 Yaoundé (Cameroon), Tel: +237699238925

Published as:

Tatang Hervé Barye, Mbey Jean Aimé, Ngally Sabouang joël Cyrill, Jacques Richard Mache, Renaud Gley, Kong Sakeo (2024), Kaolinites structural defects related to urea and dimethyl sulfoxide intercalation, *Applied Clay Science*, 255, 107415, https://doi.org/10.1016/j.clay.2024.107415

Abstract: In this study, the influence of the structural defects of kaolinites on the intercalation processes of urea and dimethyl sulfoxide (DMSO) is explored. Four samples of kaolins with kaolinite of varying levels of crystallinity were subjected to DMSO and Urea intercalation. Analyses including X-ray diffraction (XRD), Fourier-transform infrared (FTIR) spectroscopy, and differential scanning calorimetry coupled to gravimetric analysis (DSC-TGA) were used for characterization. From these analyses, the structural defects of the samples were evaluated using Hinckley index (*HI*), Slope Ratio (S*R*), factor P_0 and *R2* test. The change in the size of the coherent scattering domain was not influencing the number of layer per crystallite indicating a preservation of the structural order and the same intercalation mechanism for both molecules. For both urea and DMSO intercalation, the intercalation ratios (*IR*) were positively correlated to their crystallinity. This positive correlation of the *IR* to *HI* is also observed for P_0 and *SR*. The correlation to the associated defect shows that the defects due to random translation of the sheet that are associated to the *R2* factor, have almost no influence on the intercalation ratio. Hence, only defects in the plane affect the intercalation ratio and this is in line with the crystallinity influence.

Keywords: Kaolinite; Crystallinity; Structural Defects; Intercalation

1. Introduction

The development of composite materials with low environmental impact requires the use of biocompatible and/or biodegradable components. In the case of polymer-clay nanocomposites, the high specific surfaces associated with the lamellar structure of certain clays confer them a prominent position among the investigated fillers. This is particularly the case of smectites, which are easily exfoliated, ensuring their effective dispersion within polymeric matrix (Mbey et al., 2012; LeBaron et al., 1999).

Although widely available, kaolinitic clays are of less interest due to the high internal cohesion. Kaolinite is a 1:1 dioctahedral clay mineral having the ideal chemical formula of

$Al_2Si_2O_5(OH)_4$ (Ouangrawa et al., 2007; Kogure et al., 2010; Dill, 2016). The kaolinite layer consists of alternating sheets of siliceous tetrahedral unit, alumina octahedral unit and an interlayer space (Mbey et al., 2019). Apart from the asymmetry between the sheets, the interlayer space of kaolinite consists of an upper octahedral gibbsite-like surface $Al(OH)_3$ linked to a lower siliceous tetrahedral surface through hydrogen bonds (Bergaya et al., 2006). These high-energy bonds result in a close packing of layers and hinder the infiltration of molecules or ions. This cohesion, which is responsible of poor swelling properties, leads to low specific surface areas for kaolinites. Hence, for an improved use of kaolinite as reinforcing phase in nanocomposite materials, one needs to ameliorate their delamination/exfoliation through intercalation of small polar molecules within the interlayer space. Various small polar molecules have been studied for direct intercalation, with the most well-known ones being dimethyl sulfoxide (DMSO) (Johnston et al., 1984; Mbey et al., 2013), formamide (Frost et al., 2000), N-methylformamide (Makó et al., 2019), acetamide (Frost et al., 1999), hydrazine (Frost, et al., 2002), urea (Zhang et al., 2016; Elhadj & Perrin, 2021) and imidazole (Albach et al., 2020). However, it was recently demonstrated that the intercalation process is influenced by crystallochemical parameters such as crystallinity (Mbey et al., 2020), which is structure defects dependent. Also, the removal of an intercalated molecules is influenced by the polarity of solvent used (Zogo et al., 2021), indicating as a reverse that, the polarity of the intercalated molecule influence the bonding energy of the intercalated complex.

Kaolinites commonly exhibit defects related to the vacancy of one or more atoms and isomorphic substitutions. Research on this mineral indicates that the kaolinites with the fewest defects are those with the highest levels of crystallinity (Hinckley, 1962; Parker, 1969; Van Der Marel & Krohmer, 1969; Cases et al., 1982; Tchoubar et al., 1982). The most well-known of these defects are defects on the entire plane $(\vec{a}, \vec{b})$ or plane of the sheets (Hinckley, 1962;

Van Der Marel & Krohmer, 1969; Cases et al., 1982; Tchoubar et al., 1982; Brindley & Kao, 1986), defects involving random translation of the sheets stacking faults (Liétard, 1977; Hughes & Brown, 1979; Cases et al., 1982;Aparicio & Galan, 1999) and defects in the stacking of layer along the coherent scattering domain (Cases et al., 1982; Tchoubar et al., 1982; Amigo et al., 1994).

In a previous work (Mbey et al., 2020), it is shown that crystallinity influence the intercalation of DMSO. Given that, crystallinity in kaolinite is evaluated by diverse parameters which are associated to a typical defect, the present work is focused on bringing in an insight on the type of defect that mainly impact the intercalation and the relationship amount the various defects types in affecting the intercalation. The use of more than one intercalating molecule is also explored as a control for a potential bias that may arise from the intercalating molecule. To this end, intercalation is done using DMSO ($(CH_3)_2SO$) and urea ($(NH_2)_2CO$) as intercalating molecules due to their high polarity, non-toxic nature, and availability. Theoretical simulations of the intercalation mechanisms of these molecules demonstrate that the intercalation of DMSO into the interlayer space of kaolinite is primarily facilitated by stronger hydrogen bonds formed between the oxygen of the sulfonyl group (S=O) in DMSO and the hydrogen atoms of the alumina hydroxyls ($Al(O\text{-}H)_3$) in the octahedral site (Zhang et al., 2015, 2018). Other interactions such as low-energy apolar attractions between the methyl groups ($\text{-}CH_3$) of DMSO and the tetrahedral site, also persist (Zhang et al., 2018). As for urea, its retention within the interlayer space of kaolinite is ensured by the various hydrogen bonds it forms with the octahedral and tetrahedral sites. Urea possesses a carbonyl (C=O) group and two amino (NH_2) groups, establishing hydrogen bonds respectively with the hydrogens of octahedral hydroxyls and the basal oxygens of the tetrahedral sites (Kristóf et al., 2018; Zhang et al., 2017). Additionally, the nitrogen atom in

the amino group (NH_2) also forms hydrogen bonds with the hydrogen atoms of the $Al(O\text{-}H)_3$ hydroxyls.

The present work mainly focused on the understanding of the origin of the crystallinity influence on the intercalation of small polar molecules within the kaolinite interlayer. To this end, the investigation of the intercalation of urea and DMSO in four samples of kaolinites with varying crystallinity was done. The structural defects of the kaolinites was assessed using Hinckley index, Slope Ratio, P_0 and R2 tests. These parameters are evaluated from X-ray diffraction (XRD), thermal analyses (DSC-TGA) and Fourier Transform Infrared (FTIR) spectroscopy, respectively. The intercalation level achieved is analyzed regarding the influence of structural/crystallographic factors to provide insight into their relationship with the modification of layer staking and/or structural modification upon intercalation.

2. Materials and Methods:

Four kaolinitic clays samples indexed K1, K2, K3 and K4 respectively from Cameroonian localities of Etoa, Koutaba, Mayouom and from the Huber deposit in Georgia (U.S.A) (Schroeder and Shiflet, 2000; Ngon-Ngon et al., 2009; Poutouenchi et al., 2018; Mbey et al., 2019). The chemical composition from previous studies is given in Table S1 (supplementary material) and the kaolinite content in all the samples is > 55 %. The samples were wet sieved at 45 µm, dried at ambient temperature ((28 ± 1) °C) then manually crushed and sieved at 160 µm before being stored in closed glass jars. For the intercalation process analytical grade DMSO (99 % purity) and urea (98 % purity) were used.

The DMSO intercalation complexes were synthesized using the approach by Mbey et al., 2013 (Mbey et al., 2013). Different mixtures of kaolin and DMSO with a mass ratio of kaolinite to DMSO of 1:3 were prepared in the presence of 9 % (mass basis) of distilled water at ambient temperature. The mixtures were agitated in closed jars and the suspensions were left to stand for a period of 14 days before being filtered and air-dried at ambient. The dried

materials were ground before being placed in polyethylene bags and coded as K1-D, K2-D, K3-D and K4-D respectively for samples K1, K2, K3 and K4 intercalated with DMSO.

For kaolinite-urea complexes, 20 g of kaolinite and 11.7 g of crystalline urea are mixed by manual grinding in a mortar for 30 minutes and hydrated with 10 mL of distilled water. The manual grinding is chosen to avoid the particle size reduction and disordered complex structure when using mechanical grinding in a planetary mill (Mako *et al*., 2009). The resulting pastes were hermetically sealed and placed in a controlled temperature water bath at 70 °C for 30 minutes before being stored at ambient for 14 days. The obtained slurries are dried at room temperature in the laboratory, then ground before being placed in polyethylene bags and coded as K1-U, K2-U, K3-U and K4-U respectively for samples K1, K2, K3 and K4 intercalated with urea.

2.1. Fourier Transform Infrared (FTIR)

The infrared spectra of samples were acquired in diffuse reflectance mode using a BRUKER Alpha P Fourier-transform spectrometer. These spectra were recorded between 400 and 4000 cm^{-1} and obtained as an accumulation of 40 scans.

The stretching bands of outer and inner O-H of kaolinite at 3697 cm^{-1} and 3619 cm^{-1} are used for the evaluation of interlayer cohesion using the Parker's P_0 test (Parker, 1969). It is a measure of the internal cohesion resulting from the extent of hydrogen bonding between the sheets which is based on the ratio of the relative intensities of those bands (Equation 1). The better the crystallinity of a kaolinite sample, the greater the extension of H-bonding and hence a greater internal cohesion.

$$P_0 = \frac{I/I_0(3619\ \mathrm{cm^{-1}})}{I/I_0\ (3697\ \mathrm{cm^{-1}})} \qquad \text{(Equation 1)}$$

Where I/I_0 refers to the relative intensity of the corresponding band on the FTIR spectra.

2.2. X-Ray Diffraction

The X-ray diffraction patterns of the kaolin powders were obtained at the University of Lorraine, using a Bruker D8 advance diffractometer equipped with a Cu Kα radiation (λ = 1.5406 Å) operating under a voltage of 40 kV and an intensity of 30 mA. The diffraction patterns were recorded at a step size of 0.034772° for a step time of 576 seconds over a 2 theta range of 2.5° to 65°.

The size of the coherent scattering domain (D) was calculated using the full width at half maximum (height) (β) of the reflection associated to the d_{001} basal spacing and the Scherrer's equation (Equation 2) (Patterson, 1939). Assuming the same level of disordered in the direction associated to the reflection used, the coherent scattering domain is assimilated to the pseudo-crystal size (Kwimi et al., 2023).The number of layers per crystallite (NL) is obtained by dividing the coherent scattering domain thickness by the basal spacing associated to the reflection used to calculate the coherent scattering domain size. This parameter allows for the evaluation of structural changes after intercalation (Mbey et al., 2013).

$$D\ (Å) = \frac{K\lambda}{\beta \cos\theta} \qquad \text{(Scherrer's equation)} \qquad \text{(Equation 2)}$$

K = 0.89 (constant), λ = 1.5406 (Å) the X-ray wavelength

β = Reflection full width at half maximum

θ = Scattering angle

The Hinckley index (*HI*) is obtained from reflections as illustrated on Figure 1a and the calculation is done using equation 3 (Hinckley, 1962). The *HI* is used given that in all the samples, the kaolinite content is > 20 % (Supplementary material Tables S1 and S2) as recommended by Aparicio and Galán (1999) for samples containing quartz (which presence interfered with the effective value of the *HI*). From figure 1b, it is illustrated the parameters associated to the reflections that allow calculation of the *R2* factor using equation 4.The *HI* is related to the defects in the entire plane of the sheets and it is lower when the possibility of displacement of the vacant octahedral site is high (Cases et al., 1982). The closer the value of

HI is to 1, the better the material is crystallized. The *R2* allows for the evaluation of stacking faults in the $(\vec{a},\vec{b})$ plane due to random translation of sheets (Plançon & Tchoubar, 1975). The *R2* parameter increases with the absence of defects.

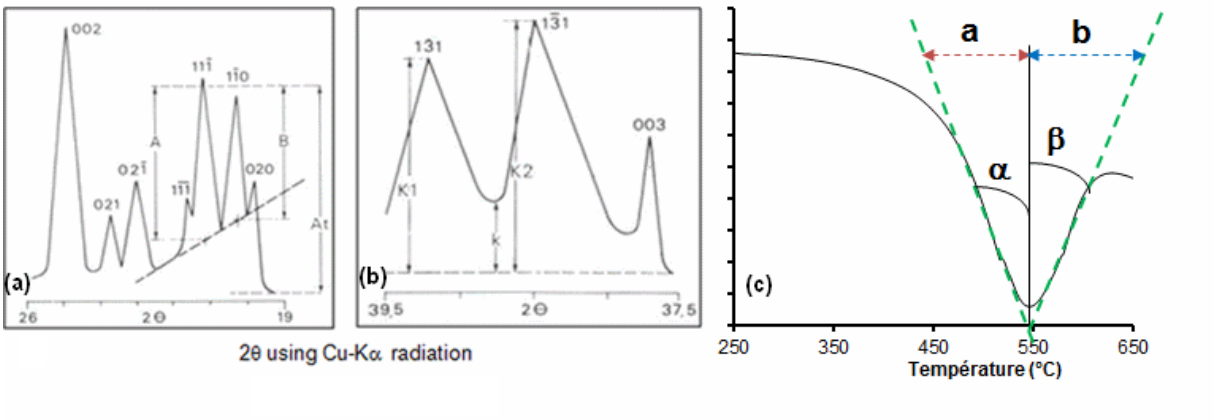

Figure 1: Calculation of *HI* (a), *R2* Factor (b) from XRD and *SR* from DSC (c)

$$HI = \frac{A+B}{A_t} \qquad \text{(Equation 3)}$$

$$R2 = \frac{1/2(K1+K2)-k}{1/3(K1+K2+k)} \qquad \text{(Equation 4)}$$

The degree of DMSO and urea intercalation into the various kaolinites was evaluated by calculating the intercalation ratios from Equation 5. This parameter is obtained using the intercalation reflection intensity and the residual Kaolinite basal reflection intensity in the kaolinite intercalated complex (Mbey et al., 2013, 2020). For this calculation, the degree of orientation of the intercalated and non-intercalated particles is assumed to be the same (Mbey et al., 2013).

$$IR = \frac{I_{001\ intercalate}}{I_{001\ intercalate} + I_{001\ Kaolinite}} \times 100 \qquad \text{(Equation 5)}$$

Here $I_{001\ intercalate}$ represents the intensity of the intercalate d_{001} reflection and $I_{001\ Kaolinite}$ represents the residual kaolinite d_{001} reflection intensity.

2.3 Thermo gravimetric analysis (TGA) and differential scanning calorimetry

Thermal analyses were conducted using a combine TGA-DSC device LINSEIS STA PT-1000. Ten milligrams (10 mg) of each sample were placed in alumina crucible and heated at a rate of 10°C/min, from room temperature to 800°C.

From the DSC curves, the band of kaolinite dehydroxylation allows the determination of a crystallinity factor related to defects in the OH plane. This factor, known as the Slope Ratio (*SR*), is determined using equation 6 and the slopes as illustrated on figure 1c. The SR is obtained as the ratio of the maximum slopes of the descending and ascending branches of the endothermic bands characterizing the dehydroxylation process (Liétard, 1977; Cases et al., 1982; Bich et al., 2009). A *SR* of 1 is associated to the absence of defects in the OH planes and indicates that water molecule diffusion out of the structure is difficult, whereas *SR* greater than 1 indicates the ease of water molecule formation and diffusion during dehydroxylation which is associated to the presence of surface defects (Liétard, 1977;Bich et al., 2009; Richard et al., 2021).

$$SR = \frac{\tan \alpha}{\tan \beta} = \frac{a}{b} \qquad \text{Equation 6}$$

3. Results and Discussion

3.1- Mineralogical Analysis of the Raw Samples

The mineralogy of the different samples shows Kaolinite as the major clay mineral with small amounts of Muscovite (Figure 2). In K2, the reflection marked T is associated to trace of smectite layers that may also include a muscovite-kaolinite interstratification (Pountouenchi et al., 2018; Mbey et al., 2019). Associated minerals included Quartz (Q), Anatase (A) and Goethite (Go).

In FTIR, the stretching vibration domain of hydroxyl groups, characteristics of kaolinitic materials, is registered at 3694 cm^{-1}, 3668 cm^{-1}, 3648 and 3620 cm^{-1} (Figure 3). For each sample, the band at 3694 cm^{-1} is attributable to in-phase stretching vibrations of O-H groups at the sheet's surface. The bands at 3668 cm^{-1} and 3648 cm^{-1} are assigned to out-of-phase

stretching vibrations of surface O-H groups in the interlayer. All the samples, except for K3, exhibit characteristic spectra of disordered kaolinites due to the almost absence of hydroxyl bands at 3668 cm^{-1}. The band at 3620 cm^{-1} is due to the stretching vibrations of inner O-H (Rouxhet et al., 1977; Mbey et al., 2019). The stretching vibrations of apical Si-O of different kaolinites are observable at around 1115 cm^{-1}, followed by the band at 998 cm^{-1}, which is assigned to Si-O-Si stretching vibrations. The deformation and translational vibration bands of Al-OH are located at 908 and 785 cm^{-1} respectively. The stretching vibration at 747 cm^{-1} is assigned to Si-O bonds (Mbey et al., 2013).

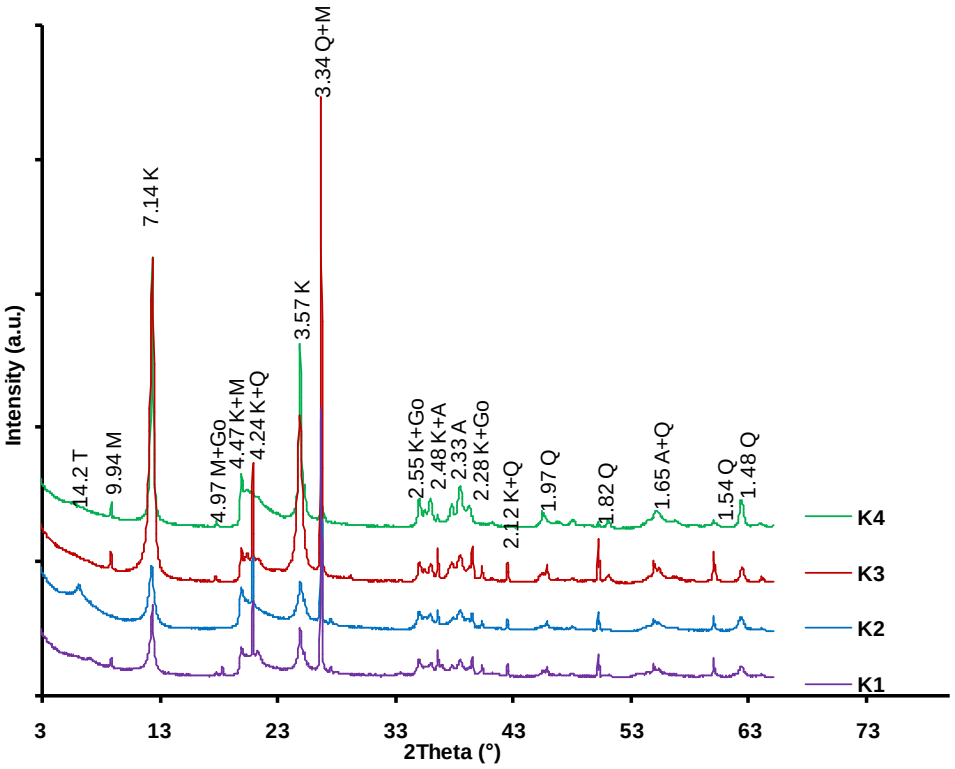

K: Kaolinite, M: Muscovite, Q: Quartz, A: Anatase, Go: Goethite, T: Interstratification

Figure 2: XRD patterns of the raw samples.

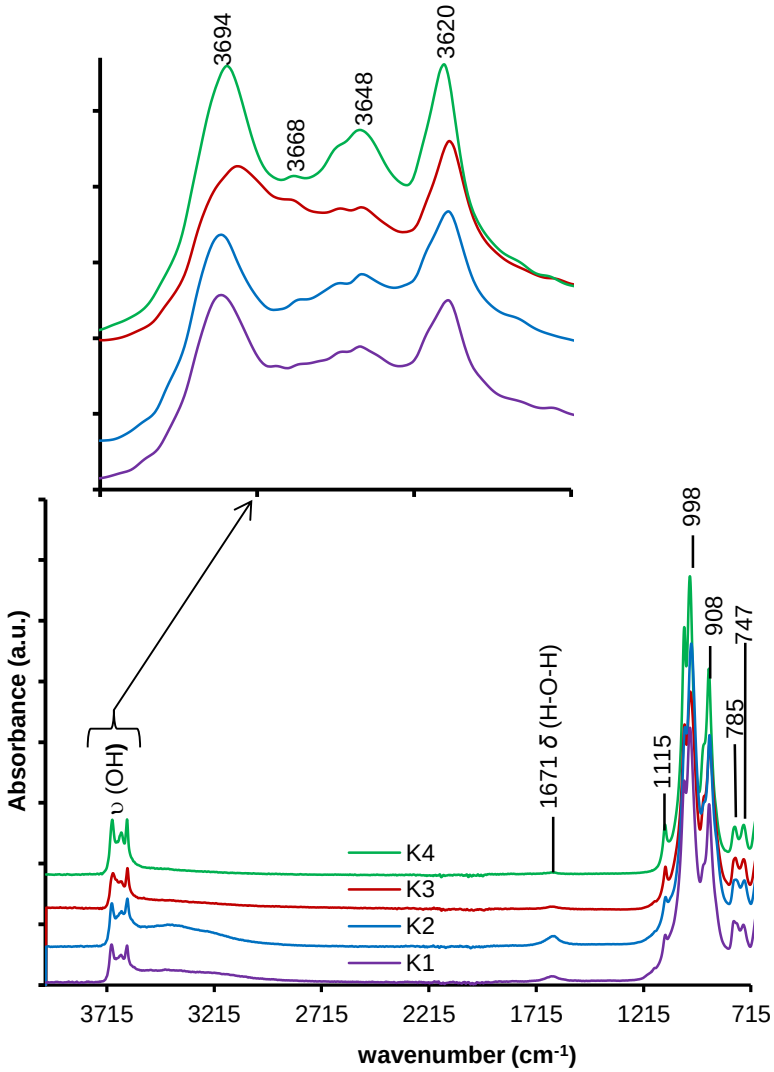

υ: Stretching vibrations ; δ: deformation vibrations.

Figure 3: FTIR spectra of raw samples.

3.2. Thermal Analysis of Raw Samples

The thermal analysis results are illustrated in figure 4. On the DSC (figure 4a) curves, the release of hydration water is observed for temperatures ≤ 100 °C in all the samples. On the K1 DSC curve, an endothermic band is observed at 270 °C, associated to goethite to hematite conversion. The endothermic bands around 500 °C in all the samples are related to the conversion of kaolinite into metakaolinite through dehydroxylation. The registered dehydroxylation temperatures are 521 °C, 519 °C, 536 °C and 543 °C respectively for K1, K2, K3 and K4. Sample K4 exhibits the highest dehydroxylation temperature, although it is

not the most crystalline, it rather has the largest particle size (D=327 Å). K3 has the better crystallinity with a relatively small size (D = 193 Å) and exhibits a high dehydroxylation temperature, although lower than K4 (Table I). This suggests that the dehydroxylation temperature of kaolinites depends not only on their crystallinity but also on their crystallite sizes. The value of the mass loss during dehydroxylation on the TGA curves (figure 4b) is less than the theoretical value for model kaolinite of 13.95 % (Ptácek et al., 2010)**.** This difference is indicative that the kaolinite molecular formulas are not ideal in the studied samples. However all the mass losses are coherent with those obtained in the study of various kaolinitic materials (Ptácek et al., 2010; Mbey et al., 2021). The order of mass losses during dehydroxylation is K1<K2<K3<K4, while the means dehydroxylation temperatures evolves as follow K2<K1<K3<K4. Both orders seem to be correlated, except for K1. It is concluded that the mean dehydroxylation temperatures is dependent on the amount of structural water in such a way that the dehydroxylation mean temperature will increase with increasing amount of structural water. The low water loss registered from K1 is most probably due to a bias in its evaluation given the presence of considerable amount of goethite. This conclusion is coherent with the fact that the more there are O-H groups in the interlayer, the higher the H-bonds intensity and hence the need of energy for dehydroxylation.

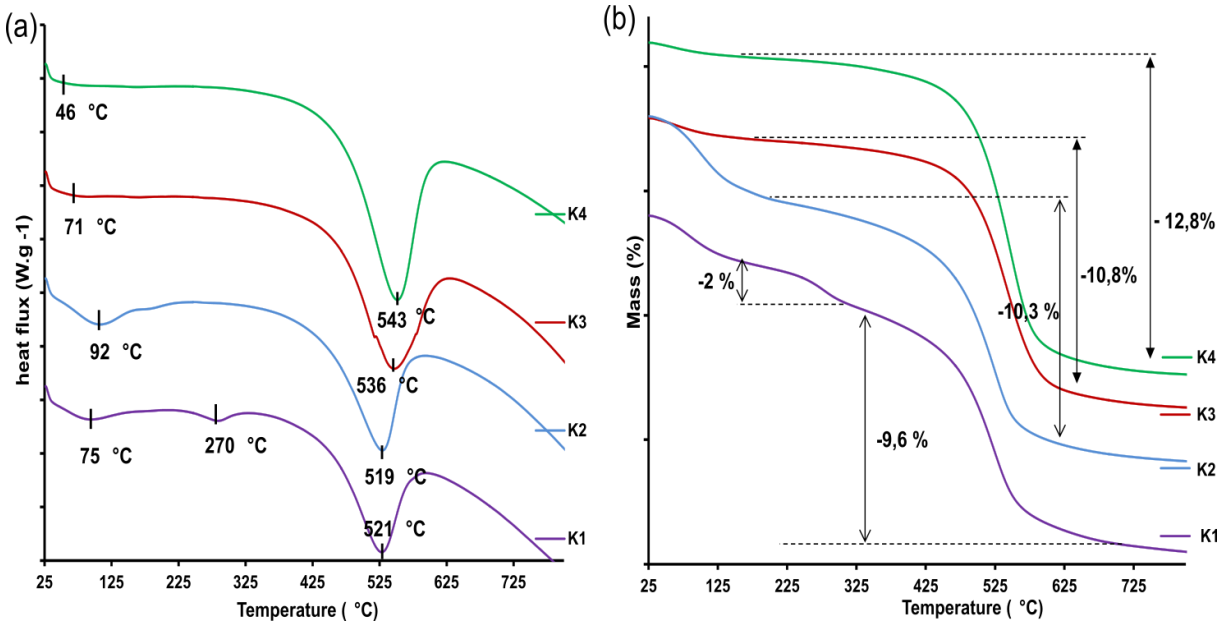

Figure 4: Thermal analysis of the kaolin samples: a) DSC; b) TGA.

3.3. Mineralogical Evolution upon Intercalation

3.3.1. DMSO intercalation

The intercalation of DMSO causes the kaolinite basal spacing d_{001} to increase from 7.15 Å to 11.15 Å (Figure 5). The basal distance variation of 4 Å is obviously associated to a monolayer intercalation of DMSO in the interlayer space of kaolinites as reported by other authors (Fang et al., 2005; Mbey et al., 2013).

The FTIR spectra of kaolinite-DMSO complexes (Figure 6) show vibration bands of C-H bonds of DMSO methyl groups at 3055, 2960, 1445, 1440 and 1352 cm^{-1}. The vibration band of the S=O sulfonyl group is observed around 950 cm^{-1}. The hydrogen bonds established between the sulfonyl of DMSO and the surface hydroxyls of the different kaolinites are confirmed by the formation of a single absorption band at 3658 cm^{-1} (Johnston et al., 1984; Mbey et al., 2013). This band intensity follows the same trend as the *IR* from XRD and also supports the idea of increase intercalation with increase crystallinity (see section 3.4).

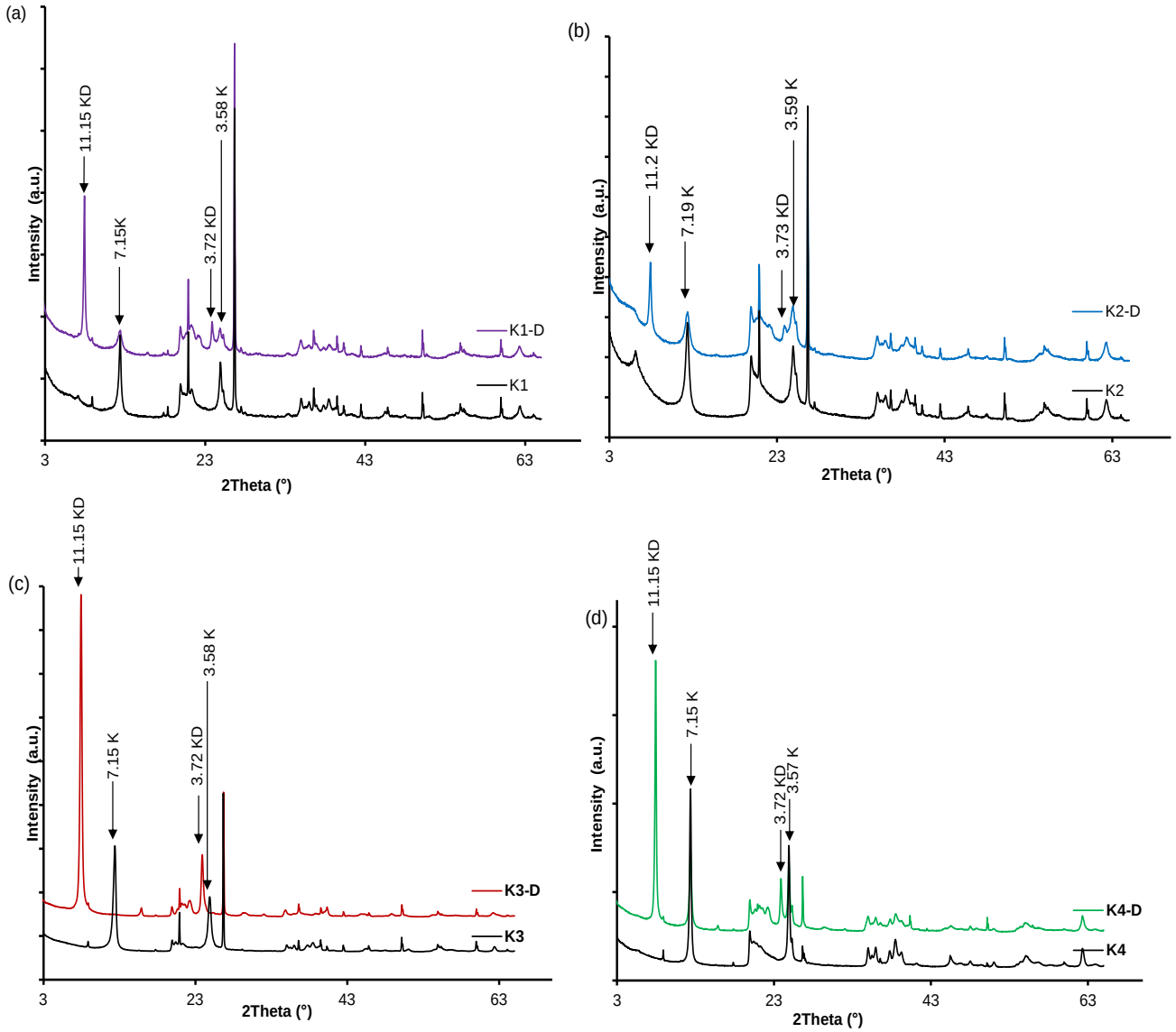

K: kaol; KD: Kaol-DMSO intercalate

Figure 5: XRD patterns of DMSO intercalated samples: a) K1; b) K2; c) K3; d) K4.

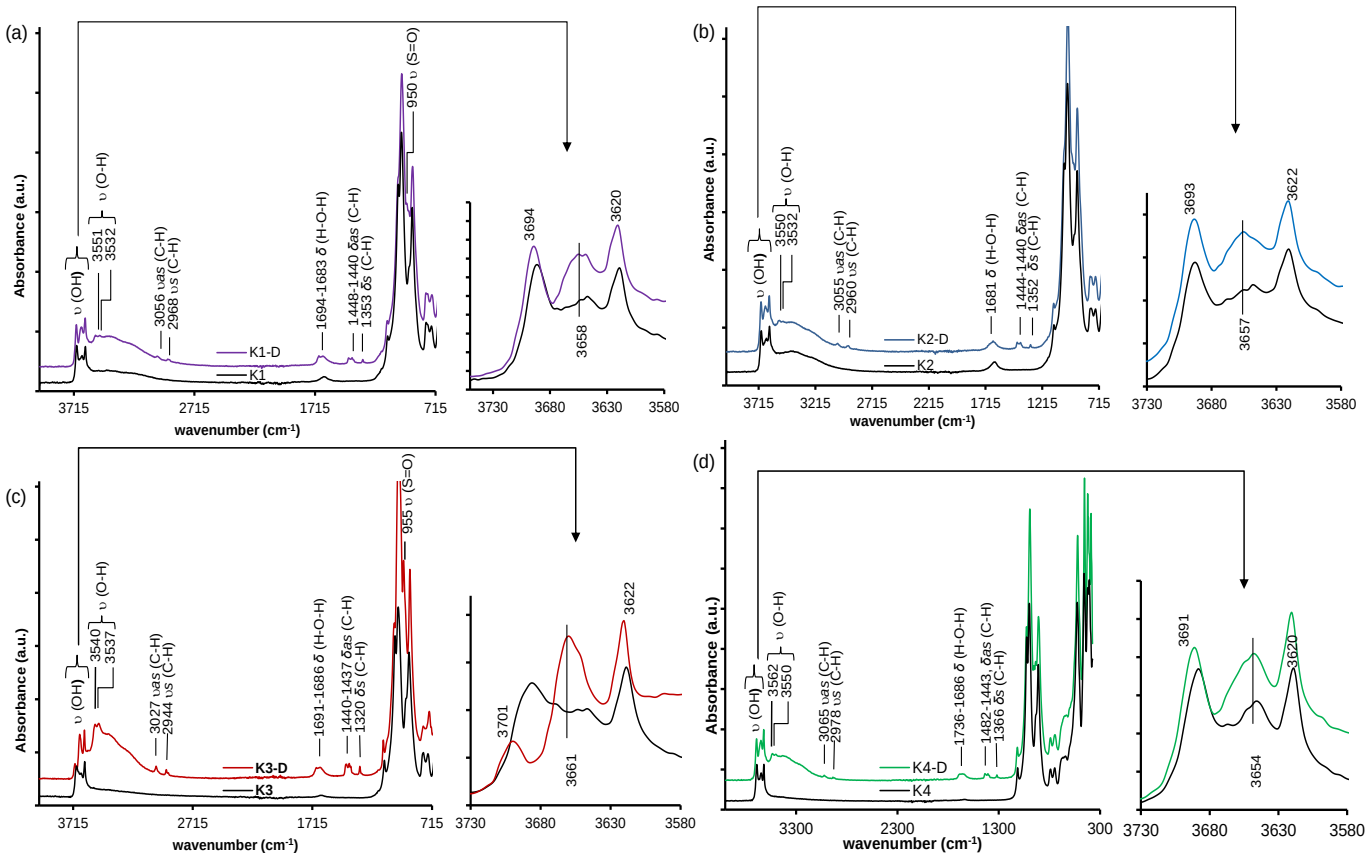

υ: Stretching vibrations ; υas: asymmetric stretching vibrations; υs: symmetric stretching vibrations; δ: deformation vibrations; δas: asymmetric deformation vibrations; δs: symmetric deformation vibrations.

Figure 6: FTIR spectra of DMSO intercalated samples: a) K1; b) K2; c) K3and d) K4.

3.3.2: Urea intercalation

The XRD of kaolinite-urea intercalated complexes is given in figure 7. It is observed that the basal spacing d_{001} change from 7.15 Å to 10.7 Å. Some characteristic reflections of urea are observed, indicating that urea is also present on the complex surface. The basal distance change upon intercalation varied is 3.55Å, which is coherent with a monolayer intercalation (Kristóf et al., 2018).

The FTIR spectra of kaolinite-urea complexes (Figure 8) highlight the interactions between kaolinites and urea and the characteristic bonds of free urea in the interlayer space of kaolinites. The N-H bonds of the amino groups of urea are manifested by stretching vibrations at 3450 and 3354 cm^{-1} and deformation at 3205, 1626 and 1598 cm^{-1}. The vibration band of the carbonyl bond C=O is assigned at 1680 cm^{-1}, while the stretching vibration bands of the

C-N bond are found at 1463 cm^{-1} and 1165 cm^{-1}. For each sample, the intensification of the band at 1626 cm^{-1} indicates the hydrogen bonds formed between the amino ($-NH_2$) groups of urea and basal Si-O oxygen atoms of the tetrahedral sites. Moreover, on the spectra of K3, a decrease of the intensity of the band at 3668 cm^{-1} and the intensification of the band towards 3655 cm^{-1} was associated to the hydrogen bonds formed between the carbonyl group of urea and the surface hydroxyls at the interlayer of the kaolinite. It is suggested that the decrease of this band intensity is not readily evidence in the other samples, due to the low amount of urea intercalated.

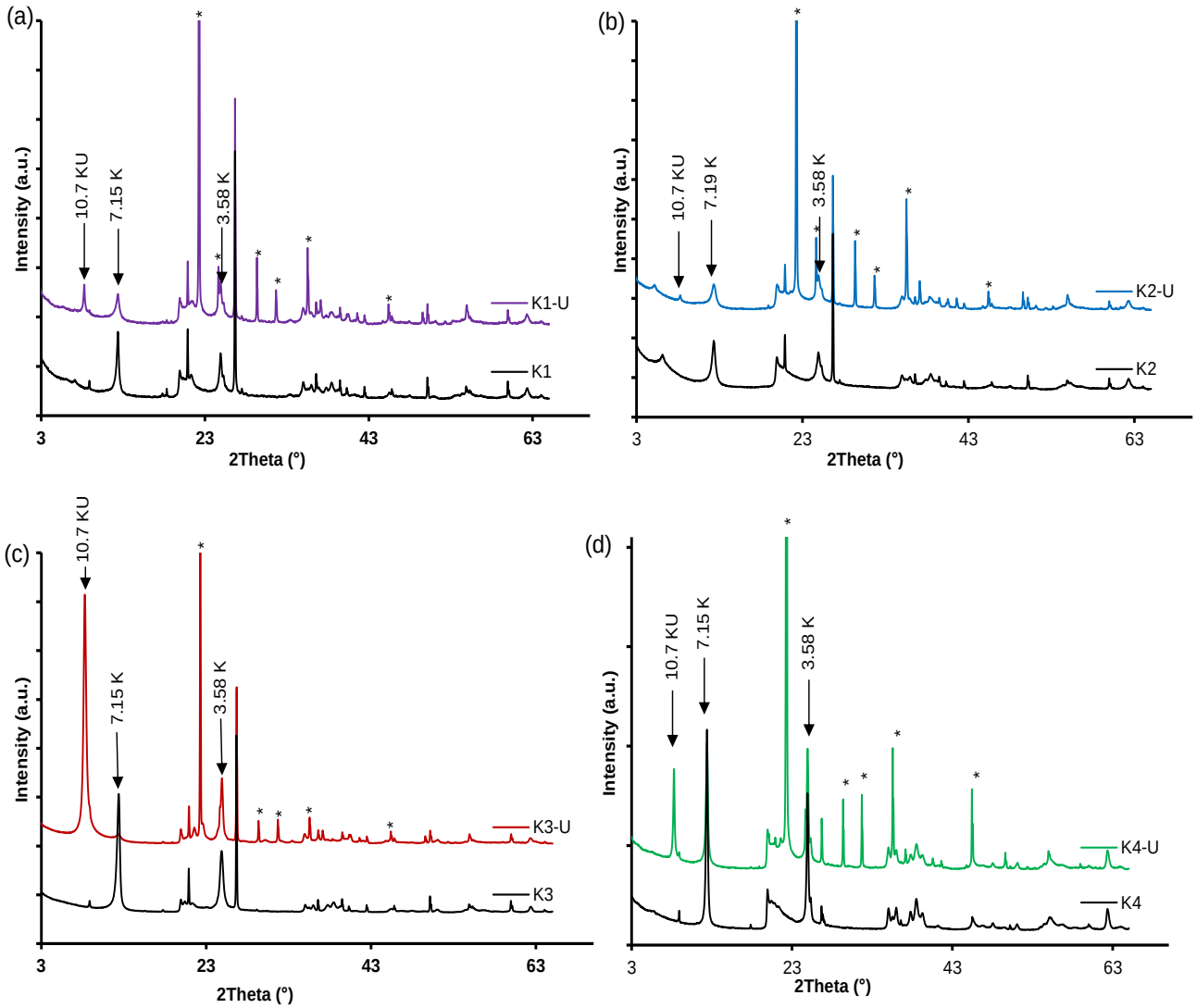

K: Kaol; KU: Kaol-urea intercalate; *****: reflections from excess surface urea

Figure 7: XRD patterns of urea intercalated samples: a) K1; b) K2; c) K3 and d) K4

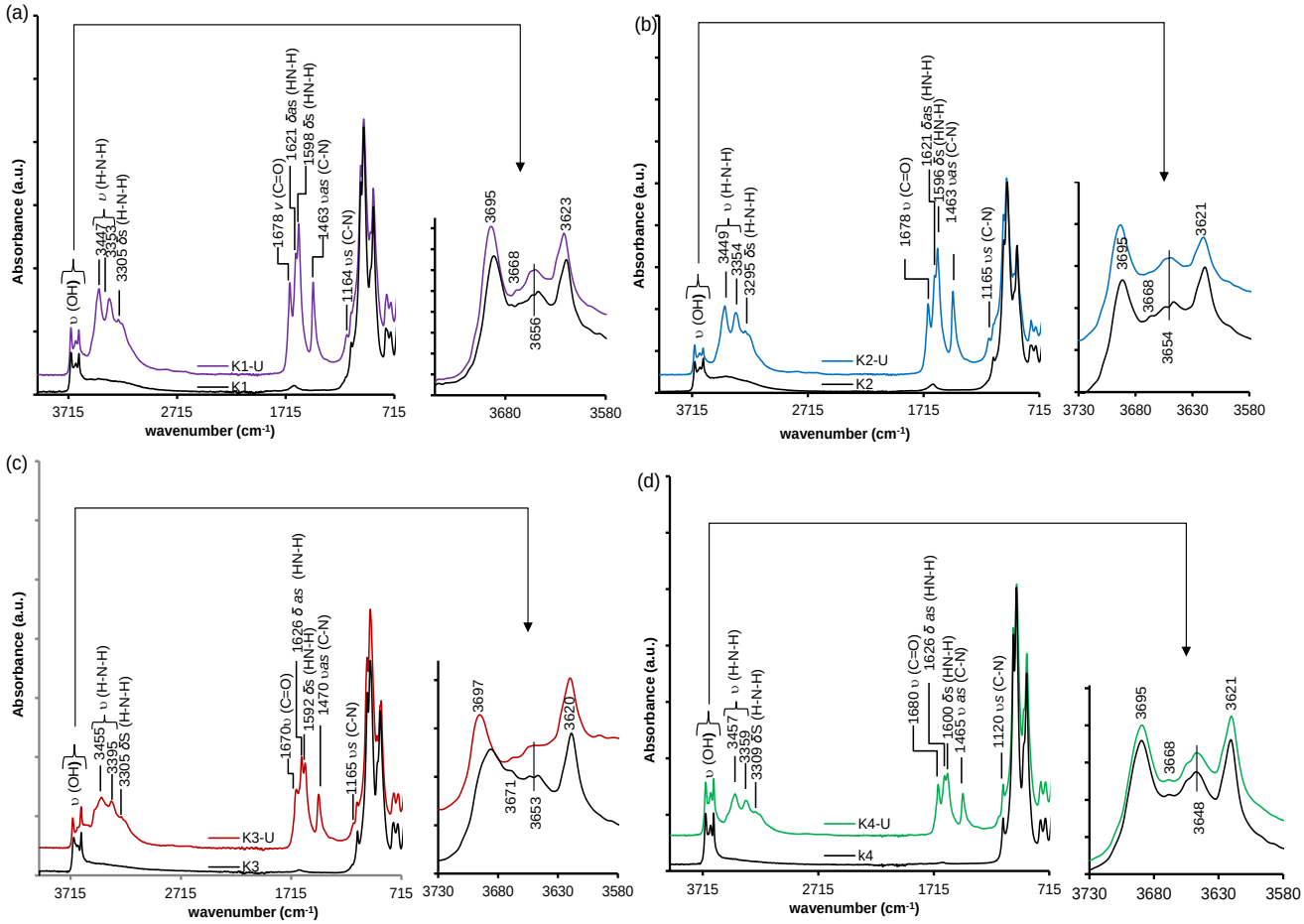

υ: Stretching vibrations ; υas: asymmetric stretching vibrations; υs: symmetric stretching vibrations; δ: deformation vibrations; δas: asymmetric deformation vibrations; δs: symmetric deformation vibrations.

Figure 8: FTIR spectra of urea intercalated samples: a) K1; b) K2; c) K3 and d) K4.

3.4. Analysis of the Structural Evolution from Raw to Intercalated Samples

The defects in the entire plane of the sheets evaluated using the Hinckley index (*HI*), lead to the following crystallinity order K3>K1>K4>K2. Sample K3 exhibits the best crystallinity (0.74) which indicates that it has fewer defects in its plane of the sheets. Although influence of quartz content on *HI* should be considered, the fact that K4 with less quartz content (see supplementary materials) have a *HI* of 0.33, the classification is sound as it is agreeing with the *SR* (Table I). Owing to the *HI* < 0.6 for kaolinite in K1, K2 and K4, they are classified as disordered kaolinite. These results are also in agreement with the observations mentioned in FTIR (section 3.1).

From the *SR* in Table I, the value closest to 1 is for sample K3 (0.92), indicating that this sample has the smallest amount of defects in the H-O plane. The cohesion order resulting from H-bonding as proposed from the SR, is the same as the crystallinity order from *HI*, which is in the following decreasing order: K3>K1>K4>K2. This agreement indicates that defects within the plane influence the H-bonding at the interlayer. It is suggested that the H-bonds are enhanced with low surface defects in the plane.

Contrary to *SR* and *HI* evolution, the *R2* factor leads to the following crystallinity order K1>K4>K3>K2. The difference here is obviously linked to the type of defects associated with each test. As *HI* is related to defects in the $(\vec{a},\vec{b})$ plane, whereas *R2* is related to random translation defects. It is then possible that the intercalation process may be favorable or not, depending on the type of defects in the kaolinite structure.

The values for P_0 (Table I) shows the following decreasing order: K3>K4>K1>K2. This order is in line with the *HI*, showing a good correlation with the internal cohesion factor P_0. The slight difference brought by the P_0 value of K4 is associated to the crystallite size of this sample, which contributes to the decrease of the internal cohesion, as also proposed by Cruz-Cumplido et al. (1982).

The intercalation ratios in the case of DMSO, lead to the following values 99 %, 83 %, 76 % and 65 % respectively for K3, K1, K4 and K2 (Table I). The intercalation order in the samples is in line with the *SR* and *HI* and the linear correlation on figure 9a is high. This observation is in accordance with the study by Mbey et al. (2020), which shows that DMSO intercalation is favored by increased crystallinity. The *R2* factor exhibits the least correlation with DMSO intercalation, whereas for P_0, the correlation is acceptable (Figure 9a). It is then suggested that DMSO intercalation is more sensitive to defect within the plane (*HI*, *SR*), whereas it is almost not sensitive to random translation defects (*R2*). The good correlation

with P_0 is then due to the fact that low defects in the plane favor cohesion and enhance the extent of H-bonding in the interlayer.

The urea intercalation ratios are 97%, 55 %; 44 % and 38 % (Table I) respectively for K3, K1, K4 and K2, leading to the same order as for DMSO intercalation. However, the levels of intercalation are lower than for DMSO and this may be due to the intercalation process used. The correlation of the intercalation ratio to the HI, SR, P_0 and R2 are given on figure 9b. As observed in the case of DMSO, low defects in the plane are more favorable to the intercalation, whereas random translation related to R2 has almost no influence. The stacking defects from random translation of the sheets do not directly affect the intercalation of urea or DMSO.

Table I: Some structural parameters of raw kaolinites and their intercalation complexes.

Samples	K1	K1-D	K1-U	K2	K2-D	K2-U	K3	K3-D	K3-U	K4	K4-D	K4-U
d_{001} (Å)	7.15	11.15	10.7	7.19	11.2	10.7	7.15	11.15	10.7	7.14	11.15	10.7
D (Å)	257	468	462	177	284	382	193	254	229	327	454	457
NL	36	42	43	25	25	36	27	23	21	46	41	43
HI	0.43	/	/	0.18	/	/	0.74	/	/	0.33	/	/
Test R2	0.94	/	/	0.57	/	/	0.65	/	/	0.66	/	/
Test P_0	0.84	/	/	0.69	/	/	1.24	/	/	0.87	/	/
SR	1.38	/	/	1.84	/	/	0.92	/	/	1.52	/	/
IR (%)	/	83	55	/	65	38	/	99	97	/	76	44

d_{001}: basal distance; *D*: Crystallite sizes; *NL*: Number of layers per crystallite; *HI*: Hinckley index; *SR*: Slope Ratio and *IR*: Intercalation Ratio.

After DMSO intercalation, the increase of coherent scattering domain (D) in all the samples approaches that of intercalated samples with urea (Table I). These nearly identical increases reflect the preservation of the stacking order and the same intercalation model. The number of layer per crystallite in the DMSO-intercalated samples is remaining almost constant in both cases. The small differences observed are due to distortions of the sheets (Mbey et al., 2020). This nearly constant structural evolution suggests a preservation of structural organization within the samples.

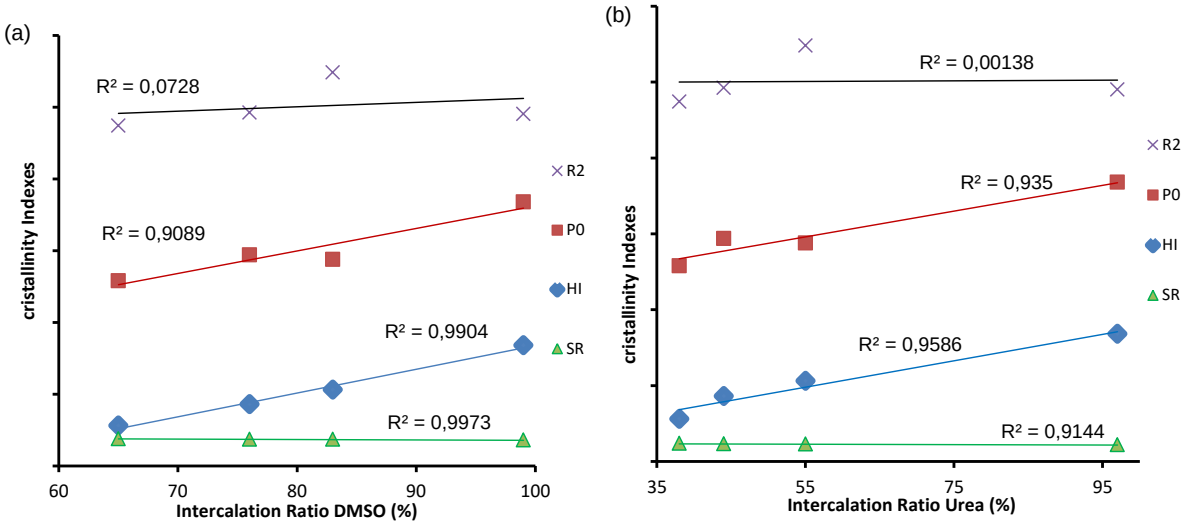

Figure 9: Plot of crystallinity indexes as a function of: a) DMSO intercalation levels; b) urea intercalation levels.

4. Conclusion

This study was focused on the assessment of the influence of the structural defects of kaolinites on the intercalation of DMSO and urea. Four kaolin samples, coded K1, K2, K3 and K4, with relative high kaolinite content were used. Their mineralogical characterization confirm the dominance of Kaolinite, sometime associated to Muscovite and trace smectite as associated clay minerals.

The Hinckley index (*HI*), the slope ratio (*SR*), the *R2* factor and the P_0 test were used as parameters related to various types of defects. Both the *HI* and the *SR* follow the same order, K3<K1<K4<K2, among the four kaolinitic samples used. This same classification is related to the fact that HI is due to defect in the plane whereas the *SR* is related to the defect in the O-H plane. The P_0 test is related to the internal cohesive forces within the distinct layers and follows the order: K3<K4<K1<K2. Regarding the *HI* or the *SR*, the P_0 ranking difference between K1 and K4 was assigned to the size of the pseudo-crystallite of each sample. Considering the R2 factor, no direct correlation to order parameters could be achieved. Given that *R2* is related to random defects due to sheets translation, such a randomization is not linkable to the order structural parameters.

The presence of the intercalated compound induces change in the H-bonding mode at the interface as revealed by the analysis of their FTIR spectra. From XRD, it is find that both urea and DMSO intercalate as monolayer within the clay structure. The change in the coherent scattering domain is coherent with a conservation of the layer stacking ordering as revealed by the number of sheet per layer, before and after intercalation. The various intercalation ratios are in order K3>K1>K4>K2. This indicates improved intercalation with increase crystallinity as indicated by the *HI*, *SR* and P_0. The correlation to various defects parameters shows that absence of defect in the plane (related to *HI* and *SR*) and optimal extent of H-bonding (P_0) at the interlayer are highly correlated to the intercalation. The R2 factor rather shows no significant correlation to other parameters and regarding the intercalation, there seems to be no influence of the *R2* on the intercalation. It is then concluded that the lesser the defect in the plane and hence the greater the extent of H-bonding, the better the intercalation within the kaolinite layer.

CRediT authorship contribution statement

Mbey Jean Aimé: Conceptualization, Methodology, Resources, Data curation, Formal analysis, Validation, Writing – review & editing, Visualization, Supervision, Funding acquisition, Project administration. **Tatang Hervé B.:** Methodology, Investigation, Data curation, Writing – original draft, Writing – review & editing, Visualization. **Ngally Sabouang C.J.:** Conceptualization, Methodology, Validation, Writing – review & editing, Visualization.

MACHE Jacques Richard: Investigation, Methodology, Resources, Data curation. **GLEY Renaud**: Investigation, Data curation, Resources. **KONG Sakeo**: Methodology, Writing – review & editing, Supervision.

Acknowledgements:

This work was partly done with resources from the *Pôle de compétences en physico-chimie de l'environnement*, ANATELo, LIEC laboratory, UMR 7360 CNRS– Université de Lorraine. The authors are thankful to Dr Isabelle BIHANNIC head of the *Pôle de compétences en physico-chimie de l'environnement*.

The Cameroonian Minister of Higher Education is acknowledge for the special research allowance to the research staff in the state Universities.

Funding: This research did not receive any specific grant from funding agencies in the public, commercial, or not-for-profit sectors

Data Availability: All the data are included in the manuscript

References

Albach, B., Liz, M. V., Prola, L. D. T., Campos, R. B., & Rampon, D. S. (2020). Eco-friendly mechanochemical intercalation of imidazole into kaolinite. *Journal of Solid State Chemistry*, *292*, 121649. https://doi.org/10.1016/j.jssc.2020.121649

Amigo, J. M., Sanz, A., Signes, M., & Serrano, J. (1994). Crystallinity of Lower Cretaceous kaolinites of Teruel (Spain). *Applied Clay Science*, *9*, 51-69. https://doi.org/10.1016/0169-1317(94)90014-0

Aparicio, P., & Galan, E. (1999). Mineralogical interference on kaolinite crystallinity Index measurements. *Clays and Clay Minerals*, *47*(1), 12-27. https://doi.org/10.1346/CCMN.1999.0470102

Bich Ch., Ambroise J., Péra J., (2009). Influence of degree of dehydroxylation on the pozzolanic activity of metakaolin. *Applied Clay sciences*, 44,194–200. https://doi.org/10.1016/j.clay.2009.01.014

Cases, J.-M., Olivier, L., Jacques, Y., & jean-François, D. (1982). Etudes des propriétés cristallochimiques, morphologiques, superficielles de kaolinites désordonnées. *bulletin de minéralogie*, *105*, 5. https://doi.org/10.3406/bulmi.1982.7566

Cruz-Cumplido, M., Sow, C., & Fripiat, J. J. (1982). Spectre infrarouge des hydroxyles, cristallinité et énergie de cohésion des kaolins. *Bulletin de Minéralogie*, *105*(5), 493-498. https://doi.org/10.3406/bulmi.1982.7570

Dill, H. G. (2016). Kaolin : Soil, rock and ore From the mineral to the magmatic, sedimentary and metamorphic environments. *Earth-Science Reviews*, *161*, 16-129. http://dx.doi.org/10.1016/j.earscirev.2016.07.003

Elhadj, M.-S. Y., & Perrin, F. X. (2021). Influencing parameters of mechanochemical intercalation of kaolinite with urea. *Applied Clay Science*, *213*, 106250. https://doi.org/10.1016/j.clay.2021.106250

Fang, Q., Huang, S., and Wang, W. (2005). Intercalation of dimethyl sulfoxide in kaolinite: Molecular dynamics simulation study. *Chemical Physics Letters*, 411, 233-237. https://doi.org/10.1016/j.cplett.2005.06.052

Frost, R. L., Kristof, J., G.N. Paroz, & Kloprogge, J. T. (1999). Intercalation of kaolinite with acetamide. *Physics and Chemistry of Minerals*, *26*, 257-263. https://doi.org/10.1007/s002690050185

Frost, R. L., Kristof, J., Horvath, E., & Kloprogge, J. T. (2000). Effect of water on the formamide-intercalation of kaolinite. *Spectrochimica Acta Part A*, *56*, 1711-1729. https://doi.org/10.1016/S1386-1425(00)00224-9

Frost, R. L., Kristof, J., Horvath, E., Martens, W. N., & Kloprogge, J. T. (2002). Complexity of Intercalation of Hydrazine into Kaolinite—A Controlled Rate Thermal Analysis and DRIFT Spectroscopic Study. *Journal of Colloid and Interface Science*, *251*, 350-359. https://doi.org/doi:10.1006/jcis.2002.8384

Hinckley, D. N. (1962). Variability in « crystallinity » values among the kaolin deposits of the coastal plain of georgia and south carolinareferences. *Eleventh National Conference on Clays and Clay Minerals*, 229-235. https://doi.org/10.1346/CCMN.1962.0110122

Hughes, J. C., & Brown, G. (1979). A crystallinity index for soil kaolins and its relation to parent rock, climate and soil maturity. *Journal of Soil Science*, *30*, 557-563. https://doi.org/10.1111/j.1365-2389.1979.tb01009.x

Johnston, C. T., Sposito, G., Bocian, D. F., & Birge, R. R. (1984). Vibrational Spectroscopic Study of the Interlamellar Kaolinite-Dimethyl Sulfoxide Complex. *Journal of Physics and Chemistry*, *88*, 5959-5964. https://doi.org/10.1021/j150668a043

Kogure, T., Elzea-Kogel, J., JOHNSTON, C. T., & BISH, D. L. (2010). Stacking disorder in a sedimentary kaolinite. *Clays and Clay Minerals*, *58*(1), 62-71. https://doi.org/10.1346/CCMN.2010.0580106

Kristóf, T., Sarkadi, Z., Ható, Z., & Gábor, R. (2018). Simulation study of intercalation complexes of kaolinite with simple amides as primary intercalation reagents. *Computational Materials Science, 143*, 118-125. https://doi.org/10.1016/j.commatsci.2017.11.010

Kwimi Tchatat, P., Ngally Sabouang, C. J., Mache, J. R., Coulibaly, S. L., Siewe, J. M., Mbey, J. A. (2023). Microwave assist synthesis of Na zeolite/hydroxysodalite from a kaolinite. Chemistry Africa, https://doi.org/10.1007/s42250-023-00745-w

LeBaron, P. C., Wang, Z., & Pinnavaia, T. J. (1999). Polymer-layered silicate nanocomposites : An overview. *Applied Clay Science, 15*, 11-29. https://doi.org/10.1016/S0169-1317(99)00017-4

Liétard, O. (1977). *Contribution à l'étude des propriétés physicochimiques, cristallographiques et morphologiques des kaolins* [Thèse de PhD en Sciences Physiques, Université de Nancy]. France, p345

Makó, É., Kovács, A., & Kristóf, T. (2019). Influencing parameters of direct homogenization intercalation of kaolinite with urea, dimethyl sulfoxide, formamide, and N-methylformamide. *Applied Clay Science, 182*, 105287. https://doi.org/10.1016/j.clay.2019.105287

Makó, É., Kristóf, J., Horváth, E., & Vágvölgyi, V. (2009). Kaolinite–urea complexes obtained by mechanochemical and aqueous suspension techniques—A comparative study. *Journal of Colloid and Interface Science, 330*, 367-373. https://doi.org/doi:10.1016/j.jcis.2008.10.054

Mbey, J.A., Ngally Sabouang, C. J., Makon, T.B., Coulibaly, S.L. & Kong, S. (2021). The thermal dehydroxylation of kaolinite using thermogravimetric analysis and Controlled rate thermal analysis. Journal of the cameroon academy of sciences, 16(3), 225-245. DOI: 10.4314/jcas.v16i3.4

Mbey, J. A., Siéwé, J. M., Sabouang, C. J. N., Razafitianamaharavo, A., Kong, S., & Thomas, F. (2020). DMSO Intercalation in Selected Kaolinites : Influence of the Crystallinity. *chemengineering*, *4*, 66. https://doi.org/doi:10.3390/chemengineering4040066

Mbey, J.A., Thomas, F., Razafitianamaharavo, A., Caillet, C. & Villieras, F., (2019). A comparative study of some kaolinites surface properties. *Applied Clay Science*, 172, 135–145.https://doi.org/10.1016/j.clay.2019.03.005

Mbey, J. A., Thomas, F., Sabouang, C. J. N., Liboum, & Njopwouo, D. (2013). An insight on the weakening of the interlayer bonds in a Cameroonian kaolinite through DMSO intercalation. *Applied Clay Science*, *83–84*, 327-335. http://dx.doi.org/10.1016/j.clay.2013.08.010

Ngon Ngon, G.F., Yongue–Fouateu, R., Bitom, D.L., Bilong, P., (2009). A geological study of clayey laterite and clayey hydromorphic material of the region of Yaoundé (Cameroon): a prerequisite for local material promotion. Journal of African Earth Sciences, 55, 69-78. https://doi.org/10.1016/j.jafrearsci.2008.12.008

Ouangrawa, M., Kamgang Kabeyene beyala, V., & Ekodeck, G. E. (2007). Cristallochimie des Kaolinites Ferrifères de Ton-Brédié (Burkina Faso). *journal of the cameroon academy of sciences*, *7*(1), 47-56.

Parker, T. W. (1969). A classification of kaolinites by infrared spectroscopy. *Clay Minerals*, *8*, 135. https://doi.org/10.1180/claymin.1969.008.2.02

Patterson, A. L. (1939). The Scherrer Formula for X-Ray Particle Size Determination. *Physical Review*, *56*, 978-982. https://doi.org/doi.org/10.1103/PhysRev.56.978

Plançon, A., & Tchoubar, M. C. (1975). Etude des Fautes d'Empilement dans les Kaolinites Partiellement Désordonnées. I. Modèle d'Empilement ne Comportant que des Fautes de translation. *journal of Applied Crystallography*, *8*, 582-588. https://doi.org/10.1107/S0021889875011429

Ptácek, P., Kubátová, D., Havlica, J., Brandstetr, J., Soukala, F., & Opravil, T. (2010). Isothermal kinetic analysis of the thermal decomposition of kaolinite : The thermogravimetric study. *Thermochimica Acta, 501*, 24-29. https://doi.org/10.1016/j.tca.2009.12.018

Pountouenchi, A., Njoya, D., Njoya, A., Rabibisao, D., Mache, J.R., Yongue, R.F., Njopwouo, D. , Fagel, N., Pilate, P. & Van Parys, L. (2018). Characterization of clays from the Foumban region (west Cameroon) and evaluation for refractory brick manufacture. *Clay Minerals*, 53 , 447 – 457. https://doi.org/10.1180/clm.2018.32

Richard, D., Martınez, J. M., Mizrahi, M., Andrini, L., Rendtorff, N. M., (2022). Assessment of structural order indices in Kaolinites: a multi-technique study including EXAFS. *Journal of Electron Spectroscopy and Related Phenomena*, 254, 147128. https://doi.org/10.1016/j.elspec.2021.147128

Rouxhet, P. G., Samudacheata, N., & Anton, H. J. O. (1977). Attribution of the OH Stretching Bands of Kaolinite. *Clay Minerals*, *12*, 171. https://doi.org/10.1180/claymin.1977.012.02.07

Schroeder, P.A., Shiflet,J. (2000).Ti-bearing phases in theHuber formation, an east Georgia kaolin deposit. *Clays and Clay Minerals*. 48(2), 151–158. https://doi.org/10.1346/CCMN.2000.0480201

Tchoubar, M. C., Plançon, A., Brahim, J. B., Clinard, C., & Sow, C. (1982). Caractéristiques structurales des kaolinites désordonnées. *Bulletin de Minéralogie*, *105*, 5. https://doi.org/10.3406/bulmi.1982.7569

Van Der Marel, H. W., & Krohmer, P. (1969). O-H Stretching Vibrations in Kaolinite, and Related Minerals. *contribution to minéralogy and petrology*, *22*, 73-82. https://doi.org/10.1007/BF00388013

Zhang, S., Liu, Q., Cheng, H., Gao, F., Liu, C., & Teppen, B. J. (2018). Mechanism responsible for intercalation of dimethyl sulfoxide in kaolinite : Molecular dynamics simulations. *Applied Clay Science*, *151*, 46-53. http://dx.doi.org/10.1016/j.clay.2017.10.022

Zhang, S., Liu, Q., Cheng, H., & Zeng, F. (2015). Combined experimental and theoretical investigation of interactions between kaolinite inner surface and intercalated dimethyl sulfoxide. *Applied Surface Science*, *331*, 234-240. http://dx.doi.org/10.1016/j.apsusc.2015.01.019

Zhang, S., Liu, Q., Gao, F., Li, X., Liu, C., Li, H., Boyd, S. A., Johnston, C. T., & Teppen, B. J. (2017). Mechanism Associated with Kaolinite Intercalation with Urea : Combination of Infrared Spectroscopy and Molecular Dynamics Simulation Studies. *The Journal of Physical Chemistry C*, *121*, 402-409. https://doi.org/10.1021/acs.jpcc.6b10533

Zogo Mfegue, B., Mbey, J. A., Onana, V. L., Coulibaly, S. L., & Ndjigui, P.-D. (2021). DMSO Deintercalation in Kaolinite–DMSO Intercalate : Influence of Solution Polarity on Removal. *Journal of Compsites Science*, *5*, 97. https://doi.org/10.3390/jcs5040097